Virus Research 339 (2024) 199260

Contents lists available at ScienceDirect

Virus Research

journal homepage: www.elsevier.com/locate/virusres

Veratramine inhibits porcine epidemic diarrhea virus entry through macropinocytosis by suppressing PI3K/Akt pathway

Huan Chen [a,b,1], Pu Zhao [a,b,1], Caisheng Zhang [a,b], Xin Ming [a,b], Chaofeng Zhang [c], Yong-Sam Jung [a,b,*], Yingjuan Qian [a,b,d,*]

[a] MOE Joint International Research Laboratory of Animal Health and Food Safety, College of Veterinary Medicine, Nanjing Agricultural University, Nanjing, Jiangsu Province, China
[b] One Health Laboratory, Jiangsu Province Foreign Expert Workstation, College of Veterinary Medicine, Nanjing Agricultural University, Nanjing, China
[c] Sino-Jan Joint Lab of Natural Health Products Research, School of Traditional Chinese Medicine, China Pharmaceutical University, Nanjing, China
[d] Jiangsu Agri-Animal Husbandry Vocational College, Veterinary Bio-Pharmaceutical, Jiangsu Key Laboratory for High-Tech Research and Development of Veterinary Biopharmaceuticals, Taizhou, Jiangsu, China

ARTICLE INFO

Keywords:
Veratramine
PEDV entry
Macropinocytosis
PI3K/Akt pathway

ABSTRACT

Porcine epidemic diarrhea (PED) is a contagious intestinal disease caused by α-coronavirus porcine epidemic diarrhea virus (PEDV). At present, no effective vaccine is available to prevent the disease. Therefore, research for novel antivirals is important. This study aimed to identify the antiviral mechanism of Veratramine (VAM), which actively inhibits PEDV replication with a 50 % inhibitory concentration (IC_{50}) of ~5 μM. Upon VAM treatment, both PEDV-nucleocapsid (N) protein level and virus titer decreased significantly. The time-of-addition assay results showed that VAM could inhibit PEDV replication by blocking viral entry. Importantly, VAM could inhibit PEDV-induced phosphatidylinositol 3-kinase/protein kinase B (PI3K/Akt) activity and further suppress micropinocytosis, which is required for PEDV entry. In addition, PI3K inhibitor LY294002 showed anti-PEDV activity by blocking viral entry as well. Taken together, VAM possessed anti-PEDV properties against the entry stage of PEDV by inhibiting the macropinocytosis pathway by suppressing the PI3K/Akt pathway. VAM could be considered as a lead compound for the development of anti-PEDV drugs and may be used during the viral entry stage of PEDV infection.

1. Introduction

Porcine epidermic diarrhea virus (PEDV) is an alphacoronavirus and belongs to the *Coronaviridae* family (Carstens and Ball, 2009; Pensaert and de Bouck, 1978). It can cause porcine epidemic diarrhea (PED), a contagious intestinal disease characterized by vomiting, diarrhea, and dehydration (Have et al., 1992; Sueyoshi et al., 1995). PED was first found in 1971 in Britain, and was first identified in the 1980s in China. In October 2010, a PEDV variant strain caused a large-scale outbreak of PED in China (Sun et al., 2012; Wang et al., 2013), resulting in tremendous economic losses (Sun et al., 2012). PEDV is an enveloped, single-stranded, positive-sense RNA virus. The PEDV genome is approximately 28 kb in length, and synthesizes four structural proteins, namely spike (S), envelope (E), membrane (M), and nucleocapsid (N), and four nonstructural proteins, namely pp1a, pp1b, and ORF3 (Bridgen et al., 1998; Kocherhans et al., 2001; Song and Park, 2012).

The PEDV lifecycle comprises different stages, such as binding, entry, replication and release. The PEDV receptor is still ambiguous and brings great difficulties in antivirals targeting receptors. At least four endocytic pathways could be used for PEDV entry, such as clathrin-mediated endocytic pathway (Abu-Eid and Ward, 2021; Fan et al., 2019; Kee et al., 2004; Wei et al., 2020), caveolae-mediated endocytic pathway, lipid raft-mediated endocytic pathway, and macropinocytosis pathway (Luo et al., 2017). Therefore, these endocytic pathways could be potential antiviral targets.

Macropinocytosis is a transient, growth factor-induced, actin-dependent endocytic pathway that leads to the internalization of fluid and membrane into large vacuoles. A lot of viruses enter the cell through the macropinocytosis pathway, such as Vaccinia virus (Huang et al., 2008; Locker et al., 2000; Mercer and Helenius, 2008), Adenovirus 2, 3,

* Corresponding authors.
E-mail addresses: ysjung@njau.edu.cn (Y.-S. Jung), yqian@njau.edu.cn (Y. Qian).
[1] These authors contributed equally to this work.

https://doi.org/10.1016/j.virusres.2023.199260
Received 24 July 2023; Received in revised form 30 October 2023; Accepted 30 October 2023

Table 1
Primer pairs used in this study.

Gene name	Sequence	
	Forward	Reverse
HLJBY-M	TTTTCGCTTTCAGCATCCTTAT	CAGTAGCAACCTTATAGCCCTCT
HLJBY-N	CTAACTTGGGTGTCAGAAAGGC	GACCCTGGTTATTTCCACGATT
HLJBY-ORF3	CAGTTGTCAAAGATGTCTCGAAGT	CTAAACAAAGCCTGCCAATAAG
Chlorocebus aethiops-Actin	ACACTGTGCCCATCTACGAGG	TTGCCAATGGTGATGACCTG

5 (Ad2, 3, 5) (Amstutz et al., 2008; Hayashi and Hogg, 2007; Meier et al., 2002; Sirena et al., 2004), Echovirus 1 (EV1) (Karjalainen et al., 2008), Coxsackievirus B (CVB) (Coyne and Bergelson, 2006; Coyne et al., 2007), Herpes simplex virus 1 (HSV1) (Nicola et al., 2005), Human immunodeficiency virus (HIV) (Liu et al., 2002; Nguyen et al., 2006; Wang et al., 2008a), Rubella virus (RB) (Kee et al., 2004), and African swine fever virus (ASFV) (Sanchez et al., 2012). Blocking the macropinocytosis pathway reduces the infectivity and even wipes out the virus.

Previous studies reported that some compounds could inhibit PEDV infection and replication. Multiple targets are present for therapeutic intervention against PEDV infection, including viral entry into host cells and proteolysis of a viral polypeptide by the 3C-like serine/3C-like protease to release nonstructural proteins in host cells. For example, Quercetin 7-rhamnoside (Q7R) could inhibit PEDV during the early stage of infection in a reactive oxygen species-independent manner (Choi et al., 2009; Song et al., 2011). Moreover, hypericin and other two compounds have been shown to possess inhibitory activity against PEDV by targeting 3C-like serine/3C-like protease (Shi et al., 2018; Zhang et al., 2021). Furthermore, treatment with trichlormethiazide, D-(+) biotin, and glutathione could also inhibit PEDV by binding to the N protein (Deejai et al., 2017). Although a variety of antiviral activities have been demonstrated in previous studies, antiviral activities for viral entry against PEDV have not been reported yet.

Veratramine (VAM) is a major *Veratrum* alkaloid (Cong et al., 2008) from the lily family in United States. It has various biological activities, such as anti-hypertension, anti-tumor and anti-arrhythmia (Ho et al., 2014; Kim et al., 2022; Sanchez and Ruiz, 2005; Thron and McCann, 1998; Wang et al., 2008b; Yin et al., 2020). This study aimed to examine the antiviral effects of VAM during PEDV infection, including HLJBY and CV777 strains. HLJBY strain belongs to G2b genotype (variant strains) (Huan et al., 2020) and CV777 belongs to G1a genotype (classical strains). VAM was found to significantly inhibit PEDV infection in a dose-dependent manner. Finally, the results demonstrated that the phosphatidylinositol 3 kinase/protein kinase B (PI3K/Akt) pathway along with its downstream signaling pathway, macropinocytosis, was critically associated with the antiviral effects of VAM during the PEDV viral entry stage. Overall, this study was novel in showing that VAM exhibited an inhibitory effect on PEDV. Taken together, the findings of this study provided new insights into the molecular mechanisms underlying macropinocytosis-mediated viral entry and may also guide the development of new broad-spectrum antiviral drugs.

2. Materials and methods

2.1. Cell culture

Vero-E6 and MARC-145 cells were cultured in Dulbecco's modified Eagle's medium (DMEM, Gibco) supplemented with 8 % fetal bovine serum (FBS, Gibco) and 1 % Penicillin/Streptomycin (w/v) (p/s) in a humidified 5 % CO_2 incubator at 37 °C.

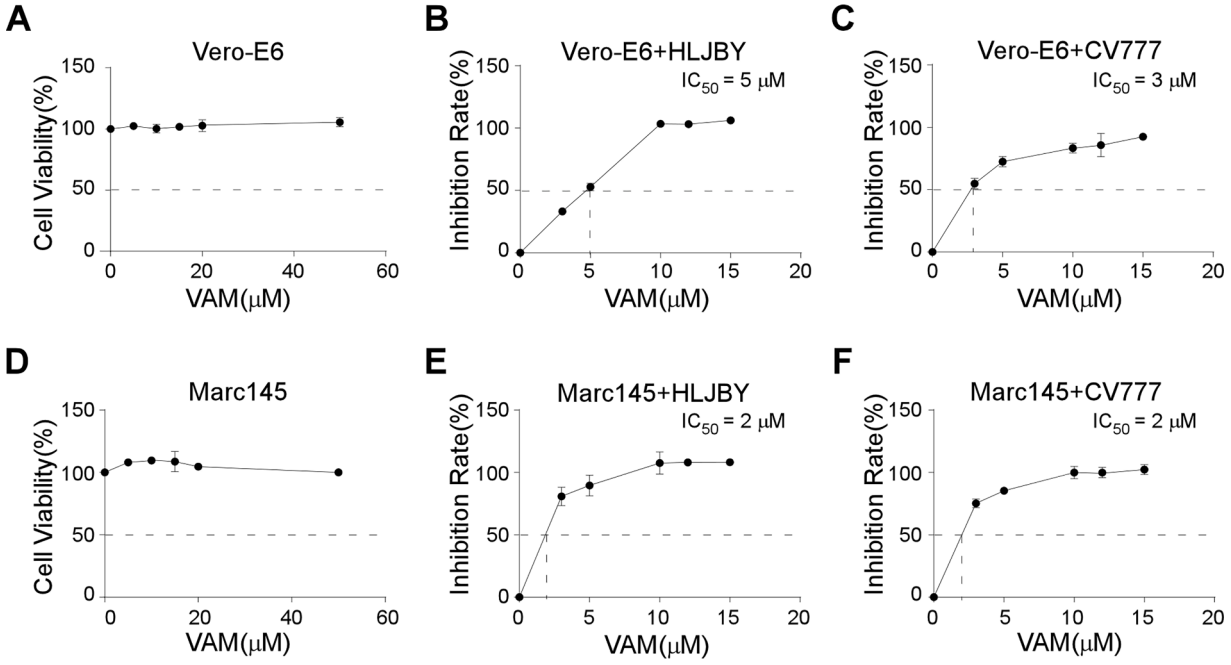

Fig. 1. Cytotoxicity and inhibition activities of VAM. (A and D) Vero-E6 or MARC-145 cells were treated with 0 μM, 5 μM, 10 μM, 15 μM, 20 μM, and 50 μM VAM for 24 h, and then treated with CCK-8 for 3 h. The OD_{450} value was measured. (B, C, E, and F) Vero-E6 or MARC-145 cells were pretreated with 0 μM, 3 μM, 5 μM, 10 μM, 12 μM, and 15 μM VAM for 2 h and infected with 1 MOI HLJBY or CV777 for 24 h. Subsequently, the cell-based ELISA assay was performed, and the OD_{450} value was measured. Data are presented as mean ± standard error of the mean (SEM) of three independent experiments.

2.2. Antibody and reagents

A rabbit anti-PEDV-N protein polyclonal antibody was generated in the laboratory. Phospho-Akt (Ser473) (D9E) and Akt (pan) (11E7) rabbit monoclonal antibodies were purchased from Cell Signaling Technology, Inc. (MA, USA). A beta actin rabbit polyclonal antibody was purchased from Proteintech Group, Inc. (IL, USA). Alexa 488-conjugated goat anti-rabbit IgG antibody and 4′,6-diamidino-2-phenylindole (DAPI) were purchased from Thermo Fisher Scientific, Inc. (MA, USA). VAM and LY294002 were purchased from Selleck Chemicals (TX, USA). We make the 10 mM stock solution with DMSO and dilute to the working solution with DMEM. A Cell Counting Kit-8 (CCK-8) was purchased from APExBio Technology, Inc. (TX, USA). A soluble TMB Substrate Solution (TMB) was purchased from Tiangen (Beijing, China). Alexa 633-conjugated transferrin (Trf), Alexa 555-conjugated Cholera Toxin subunit B (CTB), and Alexa 647-conjugated 10,000 MW Dextran (Dext) were purchased from Invitrogen (CA, USA). Nile-Red was purchased from Sigma-Aldrich (MO, USA). HiScript II Reverse Transcriptase and 2 × Taq Master Mix were purchased from Vazyme Biotech Co., Ltd. (Nanjing, China). An RNA extraction kit was purchased from PuDi Biotech Co., Ltd. (Shanghai, China).

2.3. Amplification of PEDV

Two PEDV strains (HLJBY GenBank accession no. KP403802.1 and CV777 GenBank accession no. AF353511.1) were used in this study. The Vero-E6 cells were seeded into a 10-cm dish and infected with 0.01–0.1 MOI PEDV incubated at 37 °C for 1 h. Then, sustained DMEM was changed, incubated till the cytopathic effect (CPE) was obvious, frozen and thawed three times, centrifuged supernatant was collected, and stocked into an RNase-free tube in a −80 °C freezer. The plaque assay was performed to measure the titer.

2.4. In vitro cytotoxicity assay

The cytotoxicity of VAM in vitro was measured using a CCK-8 kit according to the manufacturer's protocol. The Vero-E6 and MARC-145 cells were seeded into 96-well plates and treated with different concentrations of VAM. After 24 h, 10 μL of the CCK-8 reagent was dispensed into each well and incubated for another 4 h at 37 °C, and the OD_{450} value was measured (BioTek Instruments, Inc.).

2.5. In vitro virus inhibition assay

The cell-based enzyme-linked immunosorbent assay (ELISA) was used for in vitro virus inhibition assay. The Vero-E6 or MARC-145 cells were seeded into 96-well plates and treated with different concentrations of VAM for 2 h, and infected with 1 MOI PEDV for 24 h at 37 °C. Then, the cells were fixed and permeabilized with 4 % formaldehyde and 0.1 % Triton X-100 at 37 °C for 30 min and washed with Glycine-phosphate buffered saline (PBS) (0.02 M glycine in PBS), finally blocked with 3 % bovine serum albumin (BSA) in PBS at 37 °C for 1 h. Subsequently, the cells were incubated with the first and second antibodies, respectively. Finally, 100 μL of TMB was added, and the cells were incubated at room temperature for 20–30 min. Subsequently, 50 μL/well 2 % H_2SO_4 was dispensed to stop it, followed by a measurement of the OD_{450} value. Then, GraphPad Prism 5 was used to get the 50 % inhibitory concentration (IC_{50}) value.

2.6. Assay of the effect of VAM onPEDV binding and entry

These assays were carried out according to previous studies with minor modifications (Berry and Tse, 2017; Chen et al., 2021). For the PEDV binding assay, the Vero-E6 cells were pretreated with VAM (10 μM) for 2 h (1 h in 37 °C and another 1 h in 4 °C). They were washed with ice-cold PBS and incubated with HLJBY (1, 2, and 5 MOI) with or without VAM (10 μM) for 1 h at 4 °C. The cells were washed with ice-cold PBS to wash out the unbound virus, and then reverse transcription-polymerase chain reaction (RT-PCR) assay was performed to measure the levels of PEDV-M, PEDV-N, PEDV-ORF3 and actin mRNA. For the PEDV entry assay, the Vero-E6 cells were pretreated with VAM (10 μM) for 2 h (1 h in 37 °C and another 1 h in 4 °C), washed with ice-cold PBS to wash out compound, and then infected with HLJBY (1, 2, and 5 MOI) for 1 h at 4 °C. Then, the culture medium was replaced with a fresh medium with or without VAM (10 μM) and the cells were incubated for 2 h at 37 °C. Finally, the cells were washed with citrate buffer (pH 3) to remove non-internalized virions, and the semi-quantitative RT-PCR assay was performed to measure the levels of PEDV-M, PEDV-N, PEDV-ORF3 and actin mRNA.

2.7. Semi-quantitative RT-PCR assay

The Vero-E6 cells were seeded into six-well plates. After performing the experiments, the cellular total RNA was extracted according to the manufacturer's protocol. Then, semi-quantitative RT-PCR was performed following the manufacturer's protocol. The semi-quantitative RT-PCR primers were designed using Primer 5 software. The sequences of the primers for PEDV and cellular gene amplification are shown in Table 1.

2.8. Immunoblotting assay

The Vero-E6 and MARC-145 cells were seeded into six-well plates. When the cells were grown to 70–80 % confluence, the PEDV HLJBY and CV777 strains were inoculated into the cells. The virus-infected cells were incubated in the presence of VAM for the indicated time. Then, VAM-treated PEDV-infected or control cells were lysed in a sodium dodecyl sulfate (SDS) sample buffer (0.1 M Tris–Cl pH 6.8, 20 % Glycerine, 4 % SDS, 4 % β-Mercaptoethanol, 1 % Bromophenol Blue). Equal amounts of protein for each sample were analyzed by performing SDS-polyacrylamide gel electrophoresis (PAGE) followed by transfer to nitrocellulose filter (NC) membrane (Pall Corp.). After blocking, the membranes were incubated overnight at 4 °C with primary antibodies. Finally, the membranes were incubated with secondary antibodies for 4–6 h. Then, the membranes were visualized using the enhanced chemiluminescence (ECL) reagent (Vazyme Biotech Co., Ltd.).

2.9. Indirect immunofluorescence assay (IFA)

The Vero-E6 cells were seeded into six-well plates on coverslips. The cells on the coverslips were fixed and permeabilized with 4 % formaldehyde and 0.1 % Triton X-100 at 37 °C for 30 min. After washing with glycine-PBS (0.02 M glycine in PBS), the cells were blocked with 3 % BSA in PBS at 37 °C for 30 min. They were incubated with primary antibodies at 37 °C for 1 h, followed by washing thrice with PBS to remove unbound antibodies. Then, they were incubated with secondary antibody at 37 °C for 30 min. Unbound antibodies were removed by washing thrice with PBST. The nuclei were stained with 4′,6-diamidino-2-phenylindole (DAPI) containing the anti-fade Dabco solution. The images were obtained under a Nikon fluorescence microscope (TS100-F; DSRi2).

Table 2
Cell cytotoxicity and antiviral activity of VAM.

Name	Cell line	CC_{50} (μM)	PEDV strain	IC_{50} (μM)	SI
VAM	Vero-E6	>50	HLJBY	5	>10
			CV777	3	>17
	MARC-145	>50	HLJBY	2	>25
			CV777	2	>25

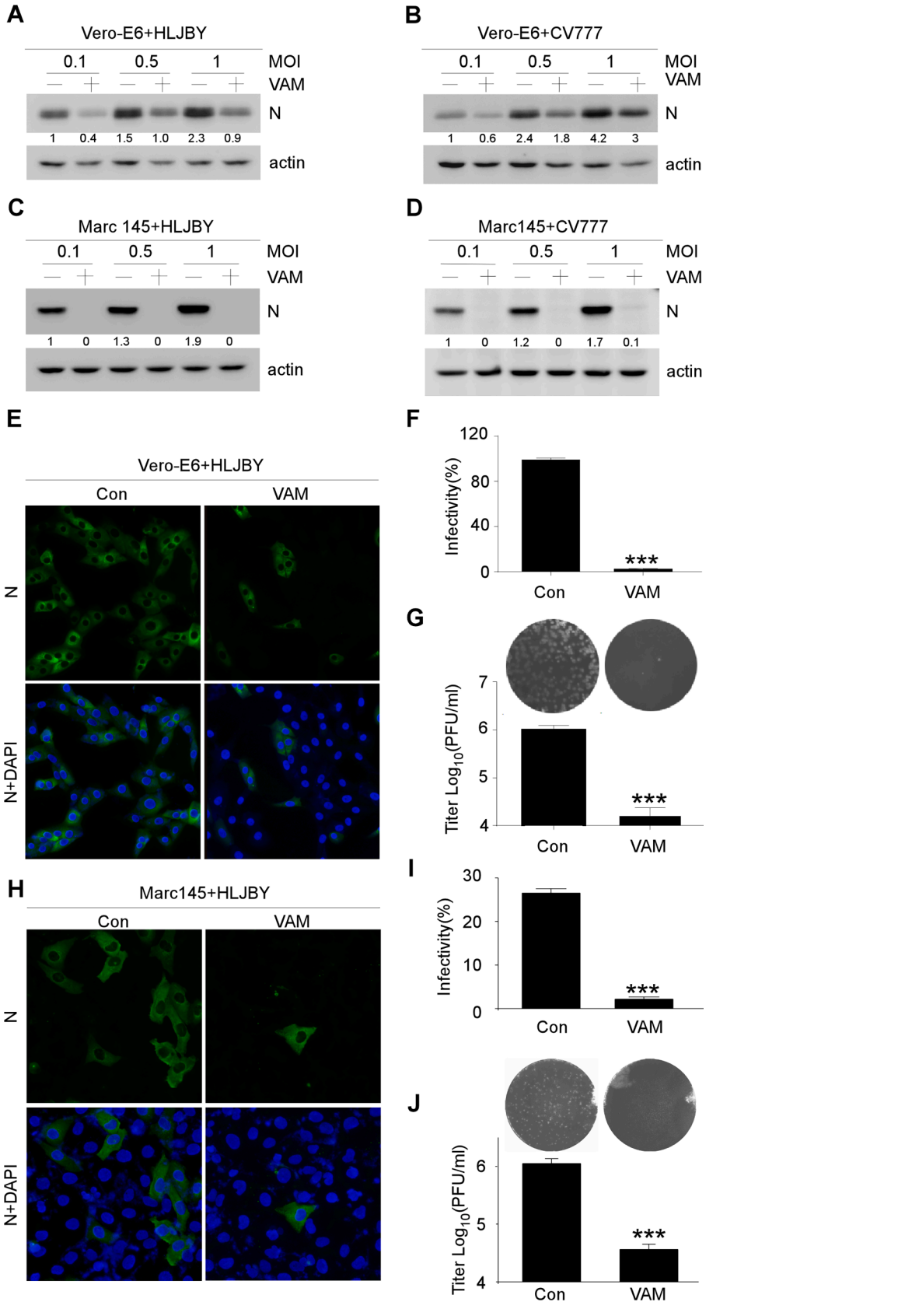

(caption on next page)

Fig. 2. Antiviral activities of VAM on PEDV. (A-D) Vero-E6 or MARC-145 cells were pretreated with 10 μM VAM for 2 h and infected with 0.1, 0.5, or 1 MOI HLJBY or CV777. After 12 hpi, the cells were harvested and immunoblotting assay was performed to determine PEDV-N and actin protein levels. (E) Vero-E6 cells were pretreated with 10 μM VAM 2 h and infected with 1 MOI HLJBY for 12 h, and then fixed and stained with the rabbit-anti-PEDV-N antibody. The nuclei were stained with DAPI. (F) HLJBY positive cells were calculated in every 200 cells randomly. (G) Vero-E6 cells were pretreated with 10 μM VAM for 2 h, and infected with 1 MOI HLJBY for 12 h. After three freeze–thaw cycles, the viral titer was determined using plaque assay on Vero-E6 cells. (H) MARC-145 cells were pretreated with 10 μM VAM for 2 h and infected with 1 MOI HLJBY for 12 h, and then fixed and stained with the rabbit-anti-PEDV-N antibody. The nuclei were stained with DAPI. (I) HLJBY positive cells were calculated in every 200 cells randomly. (J) MARC-145 cells were pretreated with 10 μM VAM for 2 h, and infected with 1 MOI HLJBY for 12 h. After three freeze–thaw cycles, the viral titer was determined using plaque assay on Vero-E6 cells. Data are presented as mean ± SEM of three independent experiments. The results were analyzed using the Student's *t* test: *, $P < 0.05$; **, $P < 0.01$; ***, $P < 0.001$. The levels of PEDV-N were normalized to the level of actin.

2.10. Plaque assay

The Vero-E6 cells were seeded into six-well plates and incubated with tenfold serial dilution (120 μL virus + 1080 μL DMEM without FBS) of PEDV at 37 °C for 1 h. Then, a 2 mL overlay medium (1 % low-melting-point agarose, 2 % FBS, and 0.0175 g/L trypsin DMEM) was added to each well, and incubated at 37 °C for about 2 days. Subsequently, 500 μL of 1 % crystal violet was added, and stained for 3–5 h in room temperature. Later, the overlay medium was removed with crystal violet and the plaque was numbered.

2.11. Statistical analysis

All experiments were performed in triplicate. All results were analyzed using GraphPad Prism 5 and were presented as means ± standard deviations (SDs). Statistical significance was determined using the two-tailed Student unpaired-sample *t*-test (*, $P < 0.05$; **, $P < 0.01$; ***, $P < 0.001$).

3. Results

3.1. Cytotoxicity and inhibition activities of VAM

In this study, a United States Food and Drug Administration-approved natural compound, VAM, was found to inhibit PEDV infection. Therefore, a cytotoxicity assay was performed. The results of the CCK-8 assay showed that the cell viabilities were more than 98 % even at 50 μM concentration in Vero-E6 cells (Fig. 1(A)). VAM showed very low cytotoxicity.

The inhibition activities were tested using the cell-based ELISA assay to evaluate the inhibitory effects of VAM on PEDV infection. Different concentrations (0 μM, 3 μM, 5 μM, 10 μM, 12 μM, and 15 μM) of VAM were used, and the percentage of inhibition was calculated. VAM showed concentration-dependent inhibition, with inhibition levels reaching more than 90 % (Fig. 1(B)). The results showed that the IC_{50}, calculated by non-linear regression, on HLJBY and CV777, were about 5 μM and 3 μM, respectively, in Vero-E6 cells (Fig. 1(B) and (C)). The same experiment was performed in MARC-145 cells to rule out the cell-type specificity. Consistent with the Vero-E6 cells, cell viabilities were also more than 98 % in MARC-145 cells (Fig. 1(D)), and the IC_{50} values were 2 μM in both HLJBY and CV777 strains (Fig. 1(E) and (F)). The 50 % cytotoxic concentration (CC_{50}) values and IC_{50} values in the Vero cells and MARC-145 cells are shown in Table 2. Thus, it was concluded that VAM had an antiviral effect against PEDV infection in multiple cell types.

3.2. Antiviral activities of VAM on PEDV

The PEDV-N protein expression was detected using Western blot analysis to confirm the inhibitory effects of VAM (Fig. 2(A)–(D)). The PEDV N protein significantly decreased by VAM in Vero-E6 cells (Fig. 2 (A) and (B)). Similarly, the PEDV N protein dramatically decreased by VAM in MARC-145 cells. Notably, the viral N protein almost could not be detected in the presence of VAM, indicating that VAM markedly inhibited PEDV infection in MARC-145 cells (Fig. 2(C) and (D)). The inhibitory effect on PEDV replication of VAM in Vero-E6 and MARC-145 cells was determined by immunofluorescence staining to further confirm the antiviral activity of VAM. The results demonstrated that the inhibitory activity against PEDV of VAM on PEDV infection was comparable as more than 90 % of the cells were not infected by PEDV when VAM was used at 10 μM (Fig. 2(E), (F) and (H), (I)). Finally, the viral titers were also determined with or without VAM treatment. The titers markedly decreased by VAM treatment both in Vero-E6 and MARC-145 cells (Fig. 2(G) and (J)). These data suggested that VAM could inhibit PEDV infection.

3.3. VAM could inhibit PEDV during the early viral entry stage

The PEDV lifecycle comprised binding, entry, replication, and release. A time-of-drug addition approach to target identification of VAM was performed to determine the stages of the virus life cycle affected by VAM. As shown in Fig. 3(A), VAM was treated during early viral entry and replication stages. The PEDV-N protein levels were significantly decreased in the binding and entry stages, and no significant difference was noted in the post-entry stage (Fig. 3(B)). In particular, the PEDV-N protein levels obviously decreased in the viral binding/entry stage-included groups, such as groups 3, 4, 5, and 8 in Immunoblot analysis (Fig. 3(B)) and groups 3, 4, and 5 in plaque assay results (Fig. 3(C)). Notably, these groups contained viral binding and entry stages. Thus, these data suggesting that VAM could inhibit PEDV binding or entry into the Vero-E6 cells.

3.4. VAM could inhibit PEDV during the entry stage

PEDV infection could be initiated by the binding of viral particles to cell surface molecules. PEDV virion binding assays were carried out as shown in Fig. 4(A) to further determine whether VAM played an essential role in initial virus binding events. The Vero-E6 cells were incubated with PEDV for 1 h at 4 °C. Thus, PEDV virion binding, but not entry, could occur. After removing unbound PEDV virions, total RNA was extracted to determine the viral levels by RT-PCR. No significant difference in PEDV binding was found between untreated and VAM-treated Vero-E6 cells (Fig. 4(B)). The RT-PCR data showed that VAM could not affect the mRNA levels of PEDV-M, PEDV-N, and PEDV-ORF3 (Fig. 4(B)). These data demonstrated that VAM was not involved in the initial binding of PEDV virions into Vero-E6 cells, indicating that VAM could act at the post-binding stage of the PEDV entry.

Next, PEDV virion entry assays were carried out as shown in Fig. 4 (C). The Vero-E6 cells were pretreated with VAM for 2 h and then infected with HLJBY for 1 h at 4 °C. The Vero-E6 cells were replaced with 37 °C prewarmed DMEM with or without VAM. After removing non-internalized PEDV virions, total RNA was extracted to determine the viral levels by RT-PCR. A significant difference in PEDV entry/internalization was found between untreated and VAM treated Vero-E6 cells (Fig. 4(D)). The RT-PCR data showed that the mRNA levels of PEDV-M, PEDV-N, and PEDV-ORF3 were significantly downregulated in VAM-treated Vero-E6 cells (Fig. 4(B)). These data demonstrated that VAM was involved in the entry/internalization of PEDV virions.

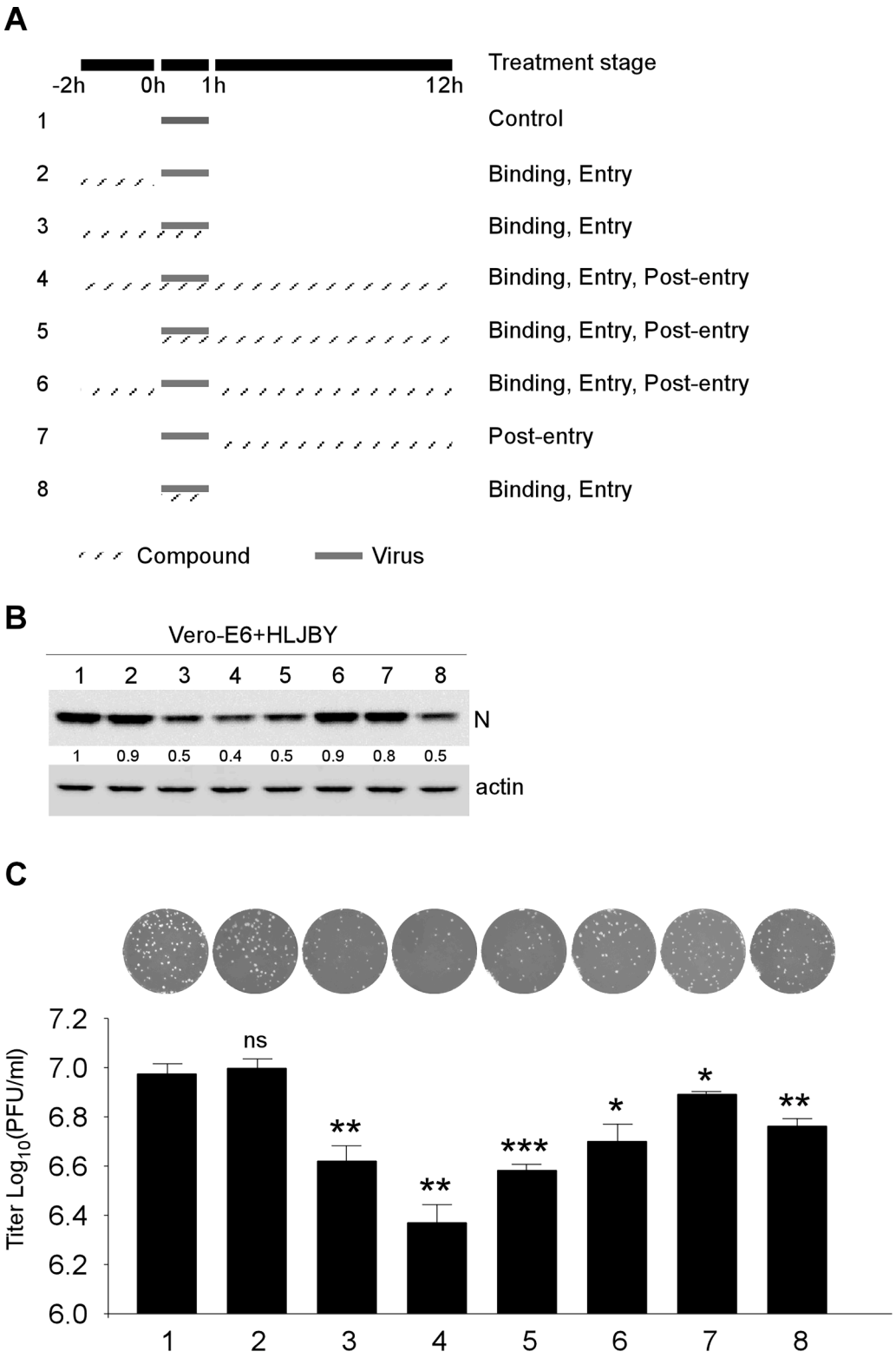

Fig. 3. Inhibitory activities of VAM against PEDV binding, entry, and post-entry stage. (A) Timeline of time of binding, entry, and post-entry assays. The gray box refers to the PEDV infection period and gray line box refers to the VAM administration. (B) After 12 hpi, the cells were harvested and immunoblotting assay was performed to determine PEDV-N and actin protein levels. (C) After 12 hpi, the cells and medium supernatant were harvested. After three freeze–thaw cycles, the viral titer was determined using plaque assay on Vero-E6 cells. The levels of PEDV-N were normalized to the level of actin.

3.5. VAM could inhibit macropinocytosis by suppressing the PI3K/Akt pathway

The endocytic pathways could be utilized by PEDV, including clathrin-mediated endocytosis, caveolae-mediated endocytosis, lipid raft-mediated endocytosis, and macropinocytosis (Luo et al., 2017; Wei et al., 2020). Considering that PEDV took advantage of different endocytic pathways to enter cells, we wondered whether VAM could affect these endocytic pathways. Thus, Trf (a marker of the clathrin-mediated endocytic pathway), CTB (a marker of the caveolae-mediated endocytic pathway), Dext (a marker of the macropinocytosis pathway), and Nile-Red (a probe of lipid) were used to determine the effect of VAM on these endocytic pathways (Al et al., 2012; Greenspan and Fowler, 1985; Greenspan et al., 1985; Li et al., 2021; Nichols, 2002; Saeed et al., 2010; Wang et al., 2010). The immunofluorescence assay showed no significant difference in Trf, CTB, and Nile-red between untreated and VAM-treated Vero-E6 cells (Fig. 5(A)). However, the signal integrity of Dext markedly decreased after VAM treatment (Fig. 5(A), right bottom panel). The results suggested that macropinocytosis could be a potential target for VAM.

Macropinocytosis could be regulated by PI3K/Akt-Rac1-p21-activated kinase 1 (PAK1) pathways (Ha et al., 2016; He et al., 2022; King and Kay, 2019; Saeed et al., 2008; Wan et al., 2021; Wang et al., 2021; Xia et al., 2019). Indeed, the PI3K/Akt pathway could be activated on PEDV infection (Kong et al., 2016). These data led us to investigate whether PI3K/Akt could be activated during PEDV infection. To test this, the Vero-E6 cells were infected with the PEDV HLJBY strain for the indicated time points. Akt activation was analyzed by monitoring Akt phosphorylation (S473) using Western blotting. Increased Akt phosphorylation was observed at early infection times (Fig. 5(B), 10–30 min). Relative phosphorylation levels of Akt returned to the baseline levels at times thereafter. Next, whether Akt phosphorylation was triggered by PEDV-host receptor interaction was further investigated. To test this, the Vero-E6 cells were infected with PEDV at 4 °C as shown in Fig. 5(C). No significant activation of Akt upon PEDV binding was observed (Fig. 5(D)). Further, VAM was found to inhibit PEDV-induced Akt phosphorylation during the early stage of PEDV infection (Fig. 5(E)), which meant that PEDV might use PI3K/Akt-dependent macropinocytosis to enter cells. PI3K/Akt specific inhibitor (LY294002) was used along with VAM to prove this conjecture, and the distribution of macropinocytosis in the cells was determined to estimate the effect of VAM on PEDV entry. The immunofluorescence results showed that the Dext fluorescence signal markedly disappeared by VAM and LY294002 treatment (Fig. 5(F)). The results suggested that VAM could inhibit PEDV entry by interfering with PI3K/Akt-dependent macropinocytosis.

3.6. VAM could negatively regulate macropinocytosis and subsequently inhibit PEDV entry

Vero-E6 cells were incubated with PEDV along with VAM or LY294002 to clarify whether VAM inhibited PEDV infection through PI3K/Akt-dependent macropinocytosis, and cell-free virus particles were removed. The levels of PEDV-N and phosphorylated Akt were measured by Western blot analysis. The phosphorylated Akt decreased by VAM and LY294002-treated cells (Fig. 6(A)). Also, the expression of PEDV N protein decreased significantly in VAM and LY294002-treated cells (Fig. 6(A)). Next, the viral titers were also determined on VAM or LY294002 treatment. The titers decreased by VAM and LY294002 (Fig. 6 (B)). Finally, PEDV internalization assay was carried out as shown in Fig. 6(C) to determine the effect of LY294002 on PEDV internalization. The semi-quantitative RT-PCR results showed that the levels of PEDV-M, PEDV-N, PEDV-ORF3 mRNA significantly decreased (Fig. 6(D)). All the aforementioned results indicated that VAM decreased PEDV entry by inhibiting PI3K/Akt-dependent macropinocytosis.

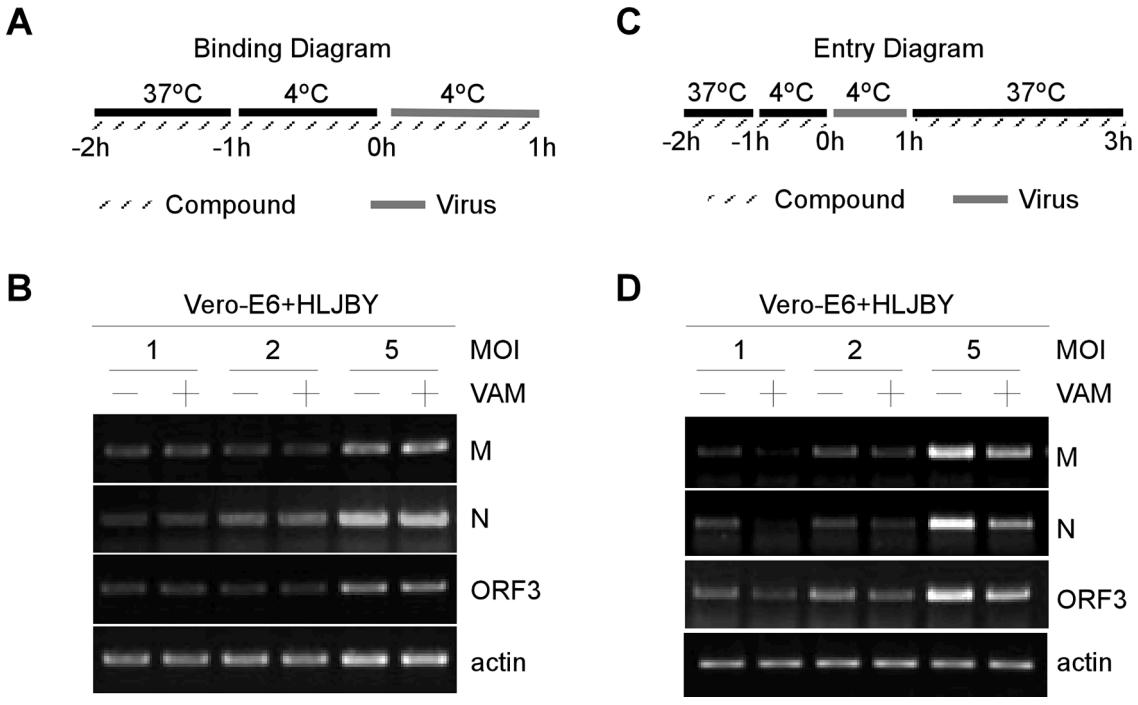

Fig. 4. VAM could inhibit PEDV during the entry stage in Vero-E6 cells. (A and B) Vero-E6 cells were pretreated with VAM (10 μM) for 2 h (1 h at 37 °C and another 1 h at 4 °C). Vero-E6 cells were incubated with HLJBY (1, 2, and 5 MOI) with or without VAM (10 μM) for 1 h at 4 °C. Cells were washed with ice-cold PBS to washout unbound virus, and then RT-PCR assay was performed to measure the levels of PEDV-M, PEDV-N, PEDV-ORF3, and actin mRNA. (C and D) Vero-E6 cells were pretreated with VAM (10 μM) for 2 h (1 h at 37 °C and another 1 h at 4 °C). The cells were then washed with ice-cold PBS and infected with HLJBY (1, 2, and 5 MOI) for 1 h at 4 °C. Then, the culture medium was replaced with a fresh medium with or without VAM (10 μM) and the cells were incubated for 2 h at 37 °C. Finally, the cells were washed with citrate buffer (pH 3) to remove non-internalized virions, and the RT-PCR assay was performed to measure the levels of PEDV-M, PEDV-N, PEDV-ORF3 and actin mRNA.

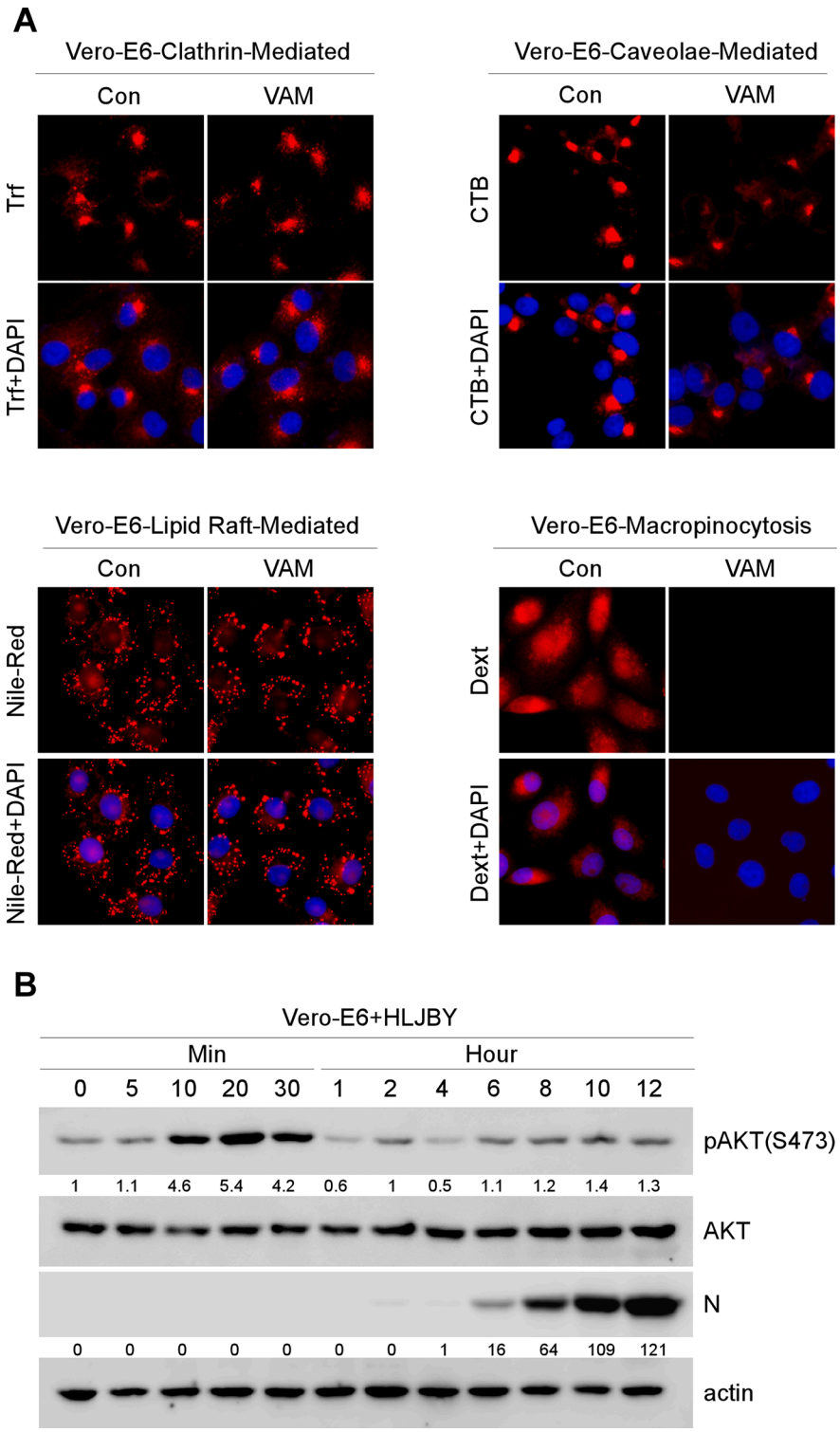

Fig. 5. VAM could inhibit micropinocytosis by suppressing the PI3K/Akt pathway. (A) Vero-E6 cells were pretreated with or without VAM (10 μM) for 2 h and treated with Trf (5 μg/mL), CTB (0.5 μg/mL), or Dext (10 μg/mL) for 1 h with or without VAM (10 μM), and then fixed. Next, nuclei were stained with DAPI to determine the effect of VAM on Trf, CTB, or Dext internalization. For lipid staining assay, Vero-E6 cells were pretreated with or without VAM (10 μM) for 2 h and then fixed and stained with Nile-Red (2 μg/mL) in 37 °C for 30 min. The nuclei were stained with DAPI to determine the effect of VAM on the lipid level. (B) Vero-E6 cells were infected with HLJBY (1 MOI), and the cells were harvested at different time points. Whole-cell extracts were prepared and analyzed by immunoblotting with the indicated antibodies. (C and D) Vero-E6 cells were pretreated at 4 °C for 1 h and then infected with HLJBY (1 MOI), and the cells were harvested at different time points. Whole-cell extracts were prepared and analyzed by immunoblotting with the indicated antibodies to determine the levels of PEDV-N and phosphorylated Akt. (E) Vero-E6 were infected with HLJBY (1 MOI) with or without VAM (10 μM) and then harvested at different time points. Then, the Western blot assay was performed to determine the levels of PEDV-N and phosphorylated Akt. (F) Vero-E6 cells were pretreated with or without VAM (10 μM) and/or LY294002 (10 μM) for 2 h and infected with HLJBY (5 MOI) and Dext (10 μg/mL), and then incubated at 37 °C for 1 h with or without VAM. Cells were fixed, and nuclei were stained with DAPI. The levels of pAKT were normalized to the level of total AKT and the levels of PEDV-N were normalized to the level of actin.

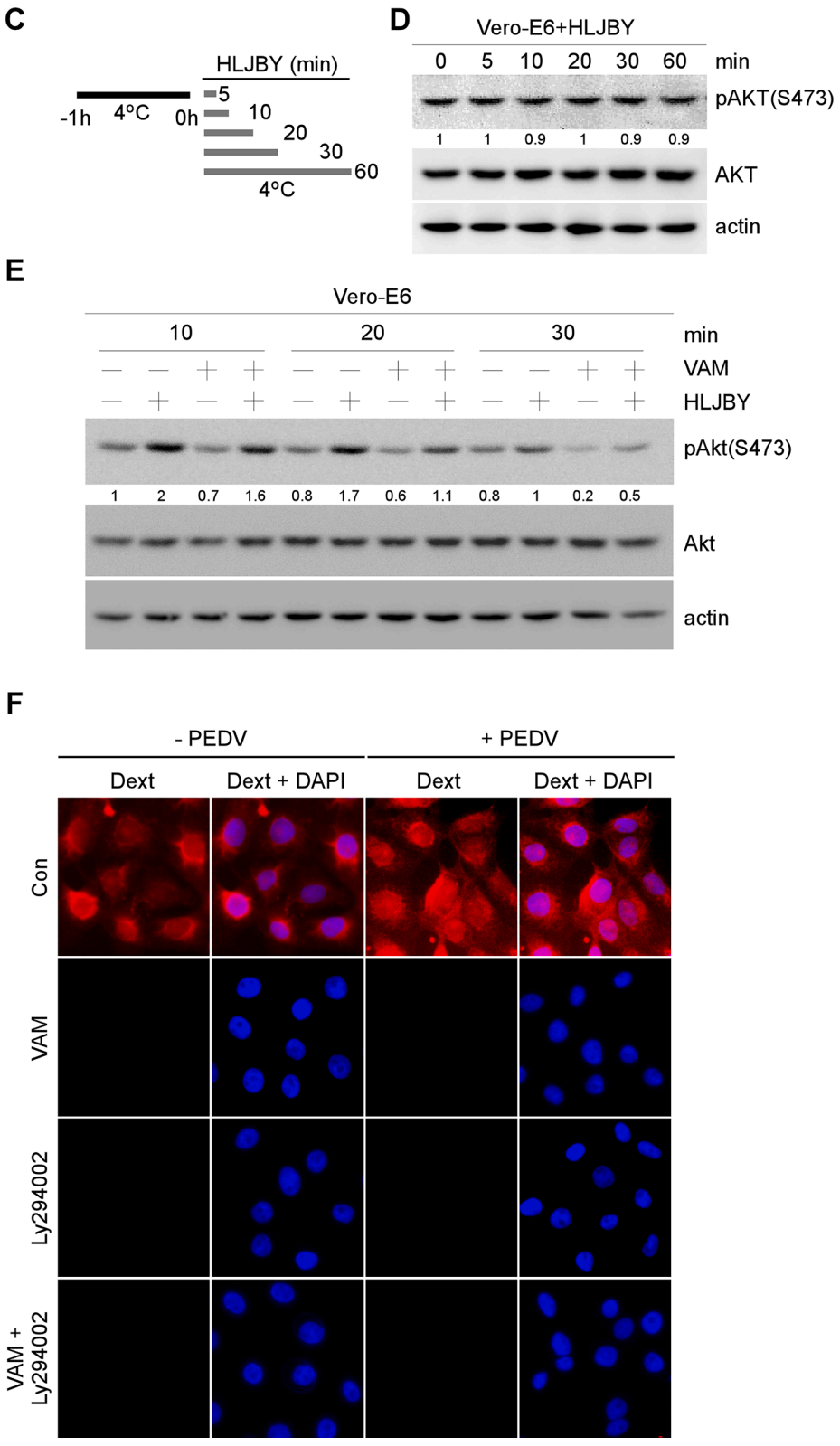

Fig. 5. (*continued*).

4. Discussion

Since first reported in Europe in 1971 (Wood, 1977), PEDV has spread and reemerged in many Asian and European countries including the United States (Lee and Lee, 2014). Large outbreaks of PED caused by various variant strains resulted in significant economic losses in the swine industry. At present, no effective drugs or vaccines are available for preventing or treating of PEDV. Therefore, antiviral drug discovery against PEDV infection remains crucial.

The replication of viruses in their host cells is first initiated by the virus binding to cell surface receptors. PEDV has been reported to use aminopeptidase N (APN) as a cellular receptor (Li et al., 2007; Liu et al.,

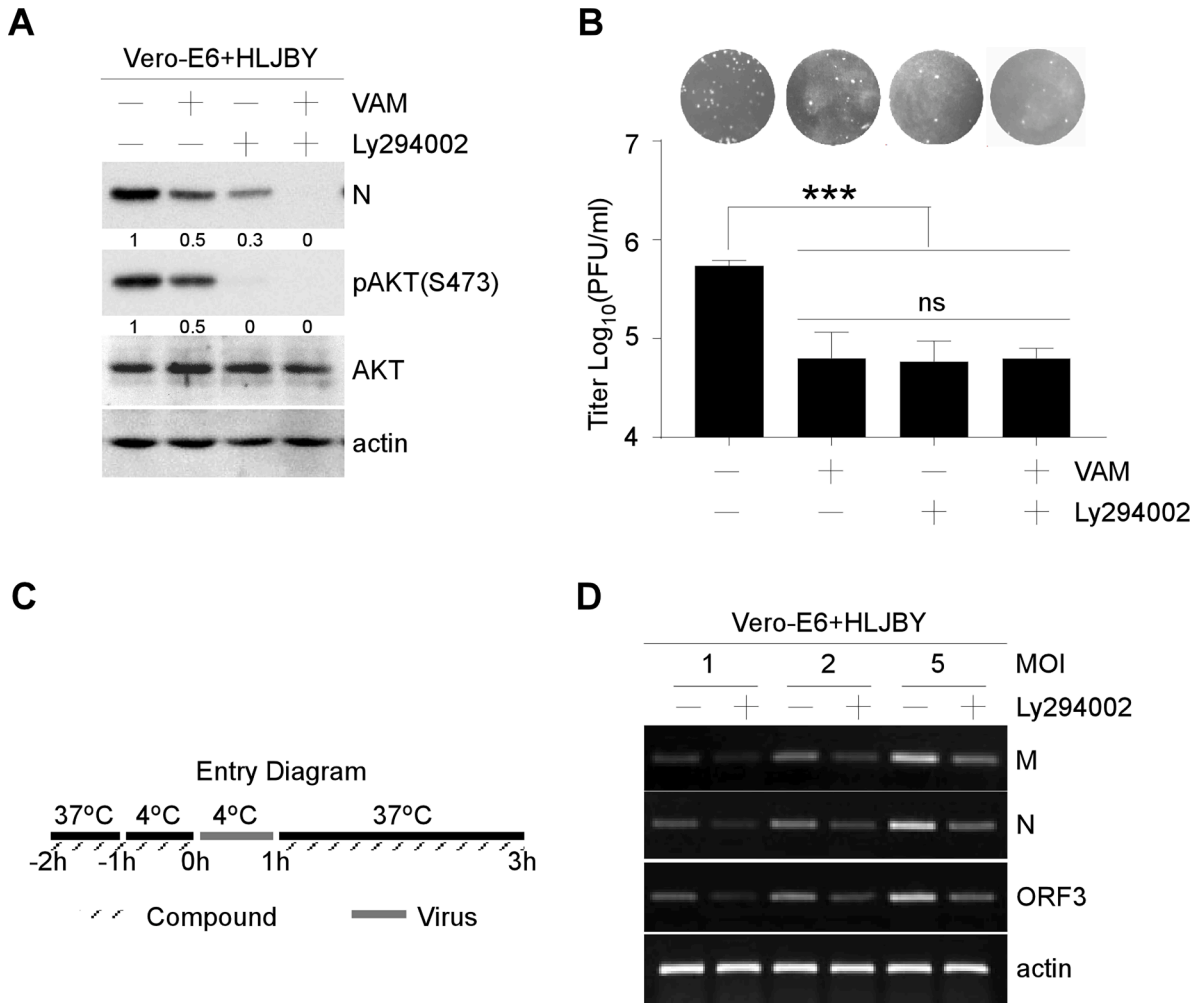

Fig. 6. PI3K/Akt pathway inhibitor LY294002 could inhibit PEDV entry into Vero-E6 cells. (A and B) Vero-E6 cells were pretreated with VAM (8 μM) and/or LY294002 (10 μM) for 2 h and infected with HLJBY (1 MOI). After 12 hpi, the cells and supernatant were harvested, and then the Western blot and PFU assays were performed with the indicated antibodies. (C and D) Vero-E6 cells were pretreated with LY294002 (10 μM) for 2 h (1 h at 37 °C and another 1 h at 4 °C). Then, the Vero-E6 cells were infected with 1, 2, or 5 MOI HLJBY at 4 °C for 1 h. The culture medium was replaced with 37 °C prewarmed DMEM with or without LY294002 (10 μM). Vero-E6 cells were washed with citrate buffer (pH 3) to remove non-internalized virions. Then, the semi-quantitative RT-PCR assay was performed to measure the levels of PEDV-M, PEDV-N, PEDV-ORF3 and actin mRNA. The levels of pAKT were normalized to the level of total AKT and the levels of PEDV-N were normalized to the level of actin.

2015; Nam and Lee, 2010). However, other data demonstrated that APN is not essential for PEDV infection. Vero cells deprived of APN were used to infect and propagate PEDV. PEDV also infects porcine APN-deleted pigs (Ji et al., 2018; Li et al., 2017; Shirato et al., 2016; Whitworth et al., 2019). Thus, whether APN acts as a receptor for PEDV entry remained controversial. This made it difficult for us to develop an antiviral drug. So far, the currently used vaccines are not affordable to control the PEDV infection. Further, no commercial drugs are available to prevent the infection. Therefore, the development of broad-spectrum antiviral would become an important strategy for preventing PEDV outbreaks. In this study, VAM was found to inhibit PEDV infection during the entry stage through the macropinocytosis pathway by suppressing the PI3K/Akt pathway in Vero-E6 cells.

In general, viral infection could regulate the activity of multiple intracellular signaling pathways, including the PI3K/Akt pathway (Diehl and Schaal, 2013). The PI3K/Akt signaling pathway is crucial in cell survival and virus replication. Previous reports showed that the porcine reproductive and respiratory syndrome virus (PRRSV) and vaccinia mature virus could also induce Akt phosphorylation during the viral entry stage (Izmailyan et al., 2012; Zhu et al., 2013). Another report showed that the PI3K/Akt pathway could be activated during PEDV infection (Kong et al., 2016). The present study showed that PEDV could activate the PI3K/Akt pathway in Vero cells at the early infection time (10–30 min) (Fig. 5(B)). No significant difference was found during the viral binding stage (Fig. 5(D)). This result indicated that the PI3K/Akt pathway could not be triggered through the PEDV-host receptor interaction. Taking these findings together, it was concluded that the PI3K/Akt pathway could be activated during both the viral early entry and viral replication stages.

Although macropinocytosis could be constitutively active in specialized cell types, it needs to be activated via signaling receptors such as receptor tyrosine kinases (RTKs) and integrins (Mercer and Helenius, 2008). Thus, macropinocytosis is transient endocytosis and could be defined as the growth factor-induced, actin-dependent endocytic process that leads to the internalization of membrane into large vesicles (i.e., macropinosome). Macropinocytosis depends on several kinases (Liberali et al., 2008). After stimulation of colony-stimulating factor-1 (CSF-1) and epidermal growth factor (EGF), the PI3K/Akt pathway could be activated and subsequently PAK1, a serine/threonine kinase, could be activated by Rac1 or Cdc42 (Burry, 1990; King and Kay, 2019). Finally, the actin rearrangement process could lead to form macropinosomes. During viral early infection, the influenza A virus

(IAV), rotavirus (RVAs) and porcine sapovirus (PSaV) could induce the endosomal acidification for viral uncoating through activating the PI3K/Akt signaling pathway (Eierhoff et al., 2010; Marjuki et al., 2011; Soliman et al., 2018a, 2018b). The degradation of macropinosomes was endo-/lysosome acidification dependent (Recouvreux and Commisso, 2017). The vacuolar proton-translocating ATPase (V-ATPase) proton pump is a multi-subunit membrane protein complex, which maintains the acidification of endosomes, lysosomes, phagosomes and Golgi-derived secretory vesicles (Coyne and Bergelson, 2006; Forgac, 2007). The cellular PI3K/Akt pathway could activate V-ATPase by directly interacting with the E subunit of V-ATPase (Collins et al., 2020; Soliman et al., 2018b). V-ATPase builds a net positive charge inside the lumen (Ohkuma et al., 1982).

VAM is a known natural steroidal alkaloid derived from plants of the lily family and exerts anticancer activities. However, the underlying mechanism remains unknown. It was postulated that VAM could prevent the release of sodium ions and make the voltage higher in the lumen. This process could inhibit the acidification of endo-/lysosome, resulting in macropinocytosis inhibition. Further studies are needed to confirm the requirement of macropinocytosis and to define the mechanism.

Severe acute respiratory syndrome–related coronavirus (SARS-CoV-2) also belongs to coronavirus and can activate the PI3K/Akt pathway during the early stage of the infection (Khezri, 2021). In the early stages of the disease, the entry and replication of the virus could be inhibited by targeting this pathway. Moreover, blocking the PI3K/Akt pathway may help eliminate the infection before it proceeds to immune dysregulation during the early stages of the immune response (Abu-Eid and Ward, 2021). Thus, VAM-mediated antiviral activity in other coronaviruses deserves further investigation.

In this study, VAM effectively suppressed PEDV infection by interfering with PI3k/Akt-mediated macropinocytosis. Overall, this study demonstrated that VAM would be a potential candidate for the development of anti-PEDV infection therapies.

CRediT authorship contribution statement

Huan Chen: Conceptualization, Data curation, Formal analysis, Funding acquisition, Investigation, Methodology, Writing – original draft. **Pu Zhao:** Data curation, Formal analysis, Investigation, Methodology, Writing – original draft. **Caisheng Zhang:** Methodology. **Xin Ming:** Conceptualization. **Chaofeng Zhang:** Conceptualization. **Yong-Sam Jung:** Conceptualization, Project administration, Supervision, Writing – review & editing. **Yingjuan Qian:** Conceptualization, Project administration, Funding acquisition, Supervision, Writing – review & editing.

Declaration of Competing Interest

The authors declare that they have no known competing financial interests or personal relationships that could have appeared to influence the work reported in this paper.

Data availability

No data was used for the research described in the article.

Acknowledgments

This work was supported by the National Natural Science Foundation of China (U19A2039, 31900141), and the Priority Academic Program Development of Jiangsu Higher Education Institutions (PAPD).

References

Abu-Eid, R., Ward, F.J., 2021. Targeting the PI3K/Akt/mTOR pathway: a therapeutic strategy in COVID-19 patients. Immunol. Lett. 240, 1–8.
Al, S.M., He, L., Peynshaert, K., Cousaert, J., Vercauteren, D., Braeckmans, K., De Smedt, S.C., Jones, A.T., 2012. siRNA and pharmacological inhibition of endocytic pathways to characterize the differential role of macropinocytosis and the actin cytoskeleton on cellular uptake of dextran and cationic cell penetrating peptides octaarginine (R8) and HIV-Tat. J. Control Release 161, 132–141.
Amstutz, B., Gastaldelli, M., Kalin, S., Imelli, N., Boucke, K., Wandeler, E., Mercer, J., Hemmi, S., Greber, U.F., 2008. Subversion of CtBP1-controlled macropinocytosis by human adenovirus serotype 3. EMBO J. 27, 956–969.
Berry, G.E., Tse, L.V., 2017. Virus binding and internalization assay for adeno-associated virus. Bio-Protocol 7. https://doi.org/10.21769/BioProtoc.2110.
Bridgen, A., Kocherhans, R., Tobler, K., Carvajal, A., Ackermann, M., 1998. Further analysis of the genome of porcine epidemic diarrhoea virus. Adv. Exp. Med. Biol. 440, 781–786.
Burry, H.C., 1990. Accident compensation: gates and gatekeepers. Med. J. Aust. 152, 450–451.
Carstens, E.B., Ball, L.A., 2009. Ratification vote on taxonomic proposals to the international committee on taxonomy of viruses (2008). Arch. Virol. 154, 1181–1188.
Chen, Y., Li, Z., Pan, P., Lao, Z., Xu, J., Li, Z., Zhan, S., Liu, X., Wu, Y., Wang, W., Li, G., 2021. Cinnamic acid inhibits Zika virus by inhibiting RdRp activity. Antivir. Res. 192, 105117 https://doi.org/10.1016/j.antiviral.2021.105117.
Choi, H.J., Kim, J.H., Lee, C.H., Ahn, Y.J., Song, J.H., Baek, S.H., Kwon, D.H., 2009. Antiviral activity of quercetin 7-rhamnoside against porcine epidemic diarrhea virus. Antivir. Res. 81, 77–81.
Collins, M.P., Stransky, L.A., Forgac, M., 2020. AKT Ser/Thr kinase increases V-ATPase-dependent lysosomal acidification in response to amino acid starvation in mammalian cells. J. Biol. Chem. 295, 9433–9444.
Cong, Y., Zhou, Y.B., Chen, J., Zeng, Y.M., Wang, J.H., 2008. Alkaloid profiling of crude and processed *Veratrum nigrum* L. through simultaneous determination of ten steroidal alkaloids by HPLC-ELSD. J. Pharm. Biomed. Anal. 48, 573–578.
Coyne, C.B., Bergelson, J.M., 2006. Virus-induced Abl and Fyn kinase signals permit coxsackievirus entry through epithelial tight junctions. Cell 124, 119–131.
Coyne, C.B., Shen, L., Turner, J.R., Bergelson, J.M., 2007. Coxsackievirus entry across epithelial tight junctions requires occludin and the small GTPases Rab34 and Rab5. Cell Host Microbe 2, 181–192.
Deejai, N., Roshorm, Y.M., Kubera, A., 2017. Antiviral compounds against nucleocapsid protein of porcine epidemic diarrhea virus. Anim. Biotechnol. 28, 120–130.
Diehl, N., Schaal, H., 2013. Make yourself at home: viral hijacking of the PI3K/Akt signaling pathway. Viruses 5, 3192–3212. https://doi.org/10.3390/v5123192.
Eierhoff, T., Hrincius, E.R., Rescher, U., Ludwig, S., Ehrhardt, C., 2010. The epidermal growth factor receptor (EGFR) promotes uptake of influenza A viruses (IAV) into host cells. PLoS Pathog. 6, e1001099.
Fan, B., Zhu, L., Chang, X., Zhou, J., Guo, R., Zhao, Y., Shi, D., Niu, B., Gu, J., Yu, Z., Song, T., Luo, C., Ma, Z., Bai, J., Zhou, B., Ding, S., He, K., Li, B., 2019. Mortalin restricts porcine epidemic diarrhea virus entry by downregulating clathrin-mediated endocytosis. Vet. Microbiol. 239, 108455.
Forgac, M., 2007. Vacuolar ATPases: rotary proton pumps in physiology and pathophysiology. Nat. Rev. Mol. Cell Biol. 8, 917–929.
Greenspan, P., Fowler, S.D., 1985. Spectrofluorometric studies of the lipid probe, nile red. J. Lipid Res. 26, 781–789.
Greenspan, P., Mayer, E.P., Fowler, S.D., 1985. Nile red: a selective fluorescent stain for intracellular lipid droplets. J. Cell Biol. 100, 965–973.
Ha, K.D., Bidlingmaier, S.M., Liu, B., 2016. Macropinocytosis exploitation by cancers and cancer therapeutics. Front. Physiol. 7, 381.
Have, P., Moving, V., Svansson, V., Uttenthal, A., Bloch, B., 1992. Coronavirus infection in mink (Mustela vison). Serological evidence of infection with a coronavirus related to transmissible gastroenteritis virus and porcine epidemic diarrhea virus. Vet. Microbiol. 31, 1–10.
Hayashi, S., Hogg, J.C., 2007. Adenovirus infections and lung disease. Curr. Opin. Pharmacol. 7, 237–243.
He, D., Xu, H., Zhang, H., Tang, R., Lan, Y., Xing, R., Li, S., Christian, E., Hou, Y., Lorello, P., Caldarone, B., Ding, J., Nguyen, L., Dionne, D., Thakore, P., Schnell, A., Huh, J.R., Rozenblatt-Rosen, O., Regev, A., Kuchroo, V.K., 2022. Disruption of the IL-33-ST2-AKT signaling axis impairs neurodevelopment by inhibiting microglial metabolic adaptation and phagocytic function. Immunity 55, 159–173 e159.
Ho, V.K., Reijneveld, J.C., Enting, R.H., Bienfait, H.P., Robe, P., Baumert, B.G., Visser, O., 2014. Changing incidence and improved survival of gliomas. Eur. J. Cancer 50, 2309–2318.
Huan, C.C., Pan, H.C., Fu, S.Y., Xu, W.Y., Gao, Q.Q., Wang, X.B., Gao, S., Chen, C.H., Liu, X.F., 2020. Characterization and evolution of the coronavirus porcine epidemic diarrhoea virus HLJBY isolated in China. Transbound. Emerg. Dis. 67, 65–79. https://doi.org/10.1111/tbed.13321.
Huang, C.Y., Lu, T.Y., Bair, C.H., Chang, Y.S., Jwo, J.K., Chang, W., 2008. A novel cellular protein, VPEF, facilitates vaccinia virus penetration into HeLa cells through fluid phase endocytosis. J. Virol. 82, 7988–7999.
Izmailyan, R., Hsao, J.C., Chung, C.S., Chen, C.H., Hsu, P.W., Liao, C.L., Chang, W., 2012. Integrin beta1 mediates vaccinia virus entry through activation of PI3K/Akt signaling. J. Virol. 86, 6677–6687. https://doi.org/10.1128/JVI.06860-11.
Ji, C.M., Wang, B., Zhou, J., Huang, Y.W., 2018. Aminopeptidase-N-independent entry of porcine epidemic diarrhea virus into Vero or porcine small intestine epithelial cells. Virology 517, 16–23.

Karjalainen, M., Kakkonen, E., Upla, P., Paloranta, H., Kankaanpaa, P., Liberali, P., Renkema, G.H., Hyypia, T., Heino, J., Marjomaki, V., 2008. A Raft-derived, Pak1-regulated entry participates in alpha2beta1 integrin-dependent sorting to caveosomes. Mol. Biol. Cell 19, 2857–2869.
Kee, S.H., Cho, E.J., Song, J.W., Park, K.S., Baek, L.J., Song, K.J., 2004. Effects of endocytosis inhibitory drugs on rubella virus entry into VeroE6 cells. Microbiol. Immunol. 48, 823–829.
Khezri, M.R., 2021. PI3K/AKT signaling pathway: a possible target for adjuvant therapy in COVID-19. Hum. Cell 34, 700–701.
Kim, D., Kwon, W., Park, S., Kim, W., Park, J.K., Han, J.E., Cho, G.J., Yun, S., Han, S.H., Kim, M.O., Ryoo, Z.Y., Choi, S.K., 2022. Anticancer effects of veratramine via the phosphatidylinositol-3-kinase/serine-threonine kinase/mechanistic target of rapamycin and its downstream signaling pathways in human glioblastoma cell lines. Life Sci. 288, 120170.
King, J.S., Kay, R.R., 2019. The origins and evolution of macropinocytosis. Philos. Trans. R. Soc. Lond. B 374, 20180158.
Kocherhans, R., Bridgen, A., Ackermann, M., Tobler, K., 2001. Completion of the porcine epidemic diarrhoea coronavirus (PEDV) genome sequence. Virus Genes 23, 137–144.
Kong, N., Wu, Y., Meng, Q., Wang, Z., Zuo, Y., Pan, X., Tong, W., Zheng, H., Li, G., Yang, S., Yu, H., Zhou, E.M., Shan, T., Tong, G., 2016. Suppression of virulent porcine epidemic diarrhea virus proliferation by the PI3K/Akt/GSK-3alpha/beta pathway. PLoS One 11, e0161508. https://doi.org/10.1371/journal.pone.0161508.
Lee, S., Lee, C., 2014. Outbreak-related porcine epidemic diarrhea virus strains similar to US strains, South Korea, 2013. Emerg. Infect. Dis. 20, 1223–1226. https://doi.org/10.3201/eid2007.140294.
Li, B.X., Ge, J.W., Li, Y.J., 2007. Porcine aminopeptidase N is a functional receptor for the PEDV coronavirus. Virology 365, 166–172.
Li, W., Luo, R., He, Q., van Kuppeveld, F.J.M., Rottier, P.J.M., Bosch, B.J., 2017. Aminopeptidase N is not required for porcine epidemic diarrhea virus cell entry. Virus Res. 235, 6–13.
Li, Y., Wang, J., Hou, W., Shan, Y., Wang, S., Liu, F., 2021. Dynamic dissection of the endocytosis of porcine epidemic diarrhea coronavirus cooperatively mediated by clathrin and caveolae as visualized by single-virus tracking. MBio 12.
Liberali, P., Ramo, P., Pelkmans, L., 2008. Protein kinases: starting a molecular systems view of endocytosis. Annu. Rev. Cell Dev. Biol. 24, 501–523. https://doi.org/10.1146/annurev.cellbio.041008.145637.
Liu, C., Tang, J., Ma, Y., Liang, X., Yang, Y., Peng, G., Qi, Q., Jiang, S., Li, J., Du, L., Li, F., 2015. Receptor usage and cell entry of porcine epidemic diarrhea coronavirus. J. Virol. 89, 6121–6125.
Liu, N.Q., Lossinsky, A.S., Popik, W., Li, X., Gujuluva, C., Kriederman, B., Roberts, J., Pushkarsky, T., Bukrinsky, M., Witte, M., Weinand, M., Fiala, M., 2002. Human immunodeficiency virus type 1 enters brain microvascular endothelia by macropinocytosis dependent on lipid rafts and the mitogen-activated protein kinase signaling pathway. J. Virol. 76, 6689–6700.
Locker, J.K., Kuehn, A., Schleich, S., Rutter, G., Hohenberg, H., Wepf, R., Griffiths, G., 2000. Entry of the two infectious forms of vaccinia virus at the plasma membane is signaling-dependent for the IMV but not the EEV. Mol. Biol. Cell 11, 2497–2511.
Luo, X., Guo, L., Zhang, J., Xu, Y., Gu, W., Feng, L., Wang, Y., 2017. Tight junction protein occludin is a porcine epidemic diarrhea virus entry factor. J. Virol. 91.
Marjuki, H., Gornitzky, A., Marathe, B.M., Ilyushina, N.A., Aldridge, J.R., Desai, G., Webby, R.J., Webster, R.G., 2011. Influenza A virus-induced early activation of ERK and PI3K mediates V-ATPase-dependent intracellular pH change required for fusion. Cell Microbiol. 13, 587–601.
Meier, O., Boucke, K., Hammer, S.V., Keller, S., Stidwill, R.P., Hemmi, S., Greber, U.F., 2002. Adenovirus triggers macropinocytosis and endosomal leakage together with its clathrin-mediated uptake. J. Cell Biol. 158, 1119–1131.
Mercer, J., Helenius, A., 2008. Vaccinia virus uses macropinocytosis and apoptotic mimicry to enter host cells. Science 320, 531–535.
Nam, E., Lee, C., 2010. Contribution of the porcine aminopeptidase N (CD13) receptor density to porcine epidemic diarrhea virus infection. Vet. Microbiol. 144, 41–50.
Nguyen, D.G., Wolff, K.C., Yin, H., Caldwell, J.S., Kuhen, K.L., 2006. ``UnPAKing'' human immunodeficiency virus (HIV) replication: using small interfering RNA screening to identify novel cofactors and elucidate the role of group I PAKs in HIV infection. J. Virol. 80, 130–137.
Nichols, B.J., 2002. A distinct class of endosome mediates clathrin-independent endocytosis to the Golgi complex. Nat. Cell Biol. 4, 374–378.
Nicola, A.V., Hou, J., Major, E.O., Straus, S.E., 2005. Herpes simplex virus type 1 enters human epidermal keratinocytes, but not neurons, via a pH-dependent endocytic pathway. J. Virol. 79, 7609–7616.
Ohkuma, S., Moriyama, Y., Takano, T., 1982. Identification and characterization of a proton pump on lysosomes by fluorescein-isothiocyanate-dextran fluorescence. Proc. Natl. Acad. Sci. USA 79, 2758–2762.
Pensaert, M.B., de Bouck, P., 1978. A new coronavirus-like particle associated with diarrhea in swine. Arch. Virol. 58, 243–247.
Recouvreux, M.V., Commisso, C., 2017. Macropinocytosis: a metabolic adaptation to nutrient stress in cancer. Front. Endocrinol. (Lausanne) 8, 261.
Saeed, M.F., Kolokoltsov, A.A., Albrecht, T., Davey, R.A., 2010. Cellular entry of Ebola virus involves uptake by a macropinocytosis-like mechanism and subsequent trafficking through early and late endosomes. PLoS Pathog. 6, e1001110.
Saeed, M.F., Kolokoltsov, A.A., Freiberg, A.N., Holbrook, M.R., Davey, R.A., 2008. Phosphoinositide-3 kinase-Akt pathway controls cellular entry of Ebola virus. PLoS Pathog. 4, e1000141.
Sanchez, E.G., Quintas, A., Perez-Nunez, D., Nogal, M., Barroso, S., Carrascosa, A.L., Revilla, Y., 2012. African swine fever virus uses macropinocytosis to enter host cells. PLoS Pathog. 8, e1002754.
Sanchez, P., Ruiz, I.A.A., 2005. In vivo inhibition of endogenous brain tumors through systemic interference of Hedgehog signaling in mice. Mech. Dev. 122, 223–230.
Shi, Y., Lei, Y., Ye, G., Sun, L., Fang, L., Xiao, S., Fu, Z.F., Yin, P., Song, Y., Peng, G., 2018. Identification of two antiviral inhibitors targeting 3C-like serine/3C-like protease of porcine reproductive and respiratory syndrome virus and porcine epidemic diarrhea virus. Vet. Microbiol. 213, 114–122.
Shirato, K., Maejima, M., Islam, M.T., Miyazaki, A., Kawase, M., Matsuyama, S., Taguchi, F., 2016. Porcine aminopeptidase N is not a cellular receptor of porcine epidemic diarrhea virus, but promotes its infectivity via aminopeptidase activity. J. Gen. Virol. 97, 2528–2539.
Sirena, D., Lilienfeld, B., Eisenhut, M., Kalin, S., Boucke, K., Beerli, R.R., Vogt, L., Ruedl, C., Bachmann, M.F., Greber, U.F., Hemmi, S., 2004. The human membrane cofactor CD46 is a receptor for species B adenovirus serotype 3. J. Virol. 78, 4454–4462.
Soliman, M., Kim, D.S., Park, J.G., Kim, J.Y., Alfajaro, M.M., Baek, Y.B., Cho, E.H., Park, C.H., Kang, M.I., Park, S.I., Cho, K.O., 2018a. Phosphatidylinositol 3-kinase/Akt and MEK/ERK Signaling pathways facilitate sapovirus trafficking and late endosomal acidification for viral uncoating in LLC-PK cells. J. Virol. 92, e01674-18.
Soliman, M., Seo, J.Y., Kim, D.S., Kim, J.Y., Park, J.G., Alfajaro, M.M., Baek, Y.B., Cho, E. H., Kwon, J., Choi, J.S., Kang, M.I., Park, S.I., Cho, K.O., 2018b. Activation of PI3K, Akt, and ERK during early rotavirus infection leads to V-ATPase-dependent endosomal acidification required for uncoating. PLoS Pathog. 14, e1006820.
Song, D., Park, B., 2012. Porcine epidemic diarrhoea virus: a comprehensive review of molecular epidemiology, diagnosis, and vaccines. Virus Genes 44, 167–175.
Song, J.H., Shim, J.K., Choi, H.J., 2011. Quercetin 7-rhamnoside reduces porcine epidemic diarrhea virus replication via independent pathway of viral induced reactive oxygen species. Virol. J. 8, 460.
Sueyoshi, M., Tsuda, T., Yamazaki, K., Yoshida, K., Nakazawa, M., Sato, K., Minami, T., Iwashita, K., Watanabe, M., Suzuki, Y., Et, A., 1995. An immunohistochemical investigation of porcine epidemic diarrhoea. J. Comp. Pathol. 113, 59–67.
Sun, R.Q., Cai, R.J., Chen, Y.Q., Liang, P.S., Chen, D.K., Song, C.X., 2012. Outbreak of porcine epidemic diarrhea in suckling piglets, China. Emerg. Infect. Dis. 18, 161–163.
Thron, C.D., McCann, F.V., 1998. Studies on the bradycardia and periodic rhythm caused by veratramine in the sinoatrial node of the guinea pig. J. Electrocardiol. 31, 257–268.
Wan, S., Ni, L., Zhao, X., Liu, X., Xu, W., Jin, W., Wang, X., Dong, C., 2021. Costimulation molecules differentially regulate the ERK-Zfp831 axis to shape T follicular helper cell differentiation. Immunity 54, 2740–2755 e2746.
Wang, J.H., Wells, C., Wu, L., 2008a. Macropinocytosis and cytoskeleton contribute to dendritic cell-mediated HIV-1 transmission to CD4+ T cells. Virology 381, 143–154.
Wang, J.T., Kerr, M.C., Karunaratne, S., Jeanes, A., Yap, A.S., Teasdale, R.D., 2010. The SNX-PX-BAR family in macropinocytosis: the regulation of macropinosome formation by SNX-PX-BAR proteins. PLoS One 5, e13763.
Wang, L., Li, W., Liu, Y., 2008b. Hypotensive effect and toxicology of total alkaloids and veratramine from roots and rhizomes of *Veratrum nigrum* L. in spontaneously hypertensive rats. Pharmazie 63, 606–610.
Wang, X.M., Niu, B.B., Yan, H., Gao, D.S., Yang, X., Chen, L., Chang, H.T., Zhao, J., Wang, C.Q., 2013. Genetic properties of endemic Chinese porcine epidemic diarrhea virus strains isolated since 2010. Arch. Virol. 158, 2487–2494.
Wang, Y., Fu, Z., Li, X., Liang, Y., Pei, S., Hao, S., Zhu, Q., Yu, T., Pei, Y., Yuan, J., Ye, J., Fu, J., Xu, J., Hong, J., Yang, R., Hou, H., Huang, X., Peng, C., Zheng, M., Xiao, Y., 2021. Cytoplasmic DNA sensing by KU complex in aged CD4(+) T cell potentiates T cell activation and aging-related autoimmune inflammation. Immunity 54, 632–647 e639.
Wei, X., She, G., Wu, T., Xue, C., Cao, Y., 2020. PEDV enters cells through clathrin-, caveolae-, and lipid raft-mediated endocytosis and traffics via the endo-/lysosome pathway. Vet. Res. 51, 10.
Whitworth, K.M., Rowland, R.R.R., Petrovan, V., Sheahan, M., Cino-Ozuna, A.G., Fang, Y., Hesse, R., Mileham, A., Samuel, M.S., Wells, K.D., Prather, R.S., 2019. Resistance to coronavirus infection in amino peptidase N-deficient pigs. Transgenic Res. 28, 21–32.
Wood, E.N., 1977. An apparently new syndrome of porcine epidemic diarrhoea. Vet. Rec. 100, 243–244. https://doi.org/10.1136/vr.100.12.243.
Xia, P., Gutl, D., Zheden, V., Heisenberg, C.P., 2019. Lateral inhibition in cell specification mediated by mechanical signals modulating TAZ activity. Cell 176, 1379–1392 e1314.
Yin, L., Xia, Y., Xu, P., Zheng, W., Gao, Y., Xie, F., Ji, Z., 2020. Veratramine suppresses human HepG2 liver cancer cell growth in vitro and in vivo by inducing autophagic cell death. Oncol. Rep. 44, 477–486.
Zhang, Y., Chen, H., Zou, M., Oerlemans, R., Shao, C., Ren, Y., Zhang, R., Huang, X., Li, G., Cong, Y., 2021. Hypericin inhibit alpha-coronavirus replication by targeting 3CL protease. Viruses 13.
Zhu, L., Yang, S., Tong, W., Zhu, J., Yu, H., Zhou, Y., Morrison, R.B., Tong, G., 2013. Control of the PI3K/Akt pathway by porcine reproductive and respiratory syndrome virus. Arch. Virol. 158, 1227–1234. https://doi.org/10.1007/s00705-013-1620-z.